NASA TECHNICAL TRANSLATION NASA TT F-14,222

EXPERIMENTAL INVESTIGATIONS OF THE ACOUSTIC REFLECTION COEFFICIENT OF DISCONTINUOUS CHANGES OF CROSS SECTION IN TUBES WITH AIR FLOW

D. Ronneberger

Translation of: Experimentelle Untersuchungen zum akustischen Reflexionsfaktor von unstetigen Querschnittsänderungen in einem luftdurchströmten Rohr", Acustica, Vol. 19, 1967-1968, pp. 222-235.

NATIONAL AERONAUTICS AND SPACE ADMINISTRATION
WASHINGTON, D.C. 20546 MARCH 1972

EXPERIMENTAL INVESTIGATIONS OF THE ACOUSTIC REFLECTION COEFFICIENT OF DISCONTINUOUS CHANGES OF CROSS SECTION IN TUBES WITH AIR FLOW

D. Ronneberger

ABSTRACT. The air flow in the region of a change of cross section is quasi-stationary at low frequencies. In this case the influence of flow velocity on the reflection coefficient of this change in cross section can be explained by the differential flow resistance. The change of the reflection coefficient is calculated in the same manner as Powell treated continuous changes of the cross section.

With increasing frequency, the influence of the pressure gradient behind the change of cross section on the reflection coefficient becomes less and less important. It is demonstrated for the example of an expansion of the cross section that at high frequencies annular vortices are separated from the cross-sectional jump in synchronism with the sound signal. These vortices produce an alternating pressure which affects the impedance of the cross-sectional jump and hence its coefficient of reflection.

1. INTRODUCTION

/222*

The reflection factor of cross section changes in tubes with flow depends on the flow velocity [1, 2, 3,]. There, as in this work also, the reflection factor of the plane ground mode is considered, at frequencies for which only this mode is capable of propagation. For continuous changes of cross section, in which the flow can be considered loss-free, Powell [2] has stated the dependence of the reflection factor on the flow velocity. He considered essentially the fact that the gradient of the static pressure at the cross section change is varied by the sonic wave, so

*Numbers in the margin indicate pagination in the original foreign text.

that it acts as an acoustic flow resistance. In [3], satisfactory agreement was found between this calculation and the measurement.

By means of this method, with which only the differential / 223
flow resistance is considered, the reflection factor of discontinuous cross section changes can also be calculated with flow superimposition. This, to be sure, is possible only at frequencies with which the flow behaves in a quasi-stationary manner. For low Mach numbers, i. e., imcompressible flow, the portion of the impedance of discontinuous cross section changes due to flow has already been determined in this way by Lutz [1]. The non-linear properties of apertures and Helmholtz resonators were also explained by means of the differential flow resistance [4, 5, 6]. In the first part of the present work, this calculation is extended to high subsonic flow velocities and compared with measurement at a perforated plate.

With frequencies at which the flow can no longer be considered as quasi-stationary in the region of the cross section jump, the differential flow resistance can also no longer be used for explanation of the change in the reflection factor caused by the flow. It is the object of the second part of this work to explore the mechanism of reflection factor change which acts at high frequencies.

SYMBOL TABLE

a	radius of the narrow tube
b	radius of the wide tube
c	adiabatic sonic velocity
f	frequency
p_g	total pressure
j	imaginary unit
k	wave number
M	Mach number

p	pressure
r_p	acoustic reflection factor
r	coordinate in the radial direction
S	cross section
t	time
v	flow velocity
x	coordinate in the axial direction
β	ratio of the phase velocity of the vortex wave and the jet velocity
γ	ratio of the specific heats
$\varkappa$	$= (\gamma - 1)/2$
ρ	density of the medium
τ	time-free phase
τ	response time of the flow
ω	rotational frequency

2. MEASURING SYSTEM

The reflection factor of the cross section changes was determined by the method of Kundt. Essentially the same measuring system as in [3] was used. The 2-meter long measuring tube with an inside diameter of 85 mm is closed off at the end with a diffusor having an almost reflection-free absorbent lining. The remaining reflection is compensated with a loudspeaker which radiates laterally into the tube at the inlet of the diffusor. Absence of standing waves at the end is the criterion for freedom from reflections. The test object is placed in the middle of the tube section. The apparatus can be operated in the frequency range from 0.3 kHz to 1.5 kHz.

A pressure chamber loudspeaker with about 50 W electrical input power placed laterally at the inlet of the measuring tube serves as the sound transmitter. In this way, sound levels of about 130 dB are attained in the tube. The standing wave field is explored with a probe microphone. The microphone is a condensor microphone which, because of its wide linearity

range, is insensitive to large changes of the static pressure with time.

The air, which is maintained at room temperature, is blown into the measuring tube through an inlet jet with a cross section ratio of 25:1 at the sound source end. The inlet jet serves simultaneously for measurement of the dynamic pressure. Flow velocities of up to 150 m/s are attained. This corresponds to a Mach number of 0.45. The cross section changes are produced by sliding appropriate bushings into the measuring tube. With the narrow cross section, the maximum Mach number attainable is 0.6 to 0.7.

The output voltage of the microphone passes a narrow-band filter (10 Hz bandwidth) and is recorded on a recorder along with location marks, so that one can read from the charts the amount and phase of the reflection factor. The sonic pressure can also be recorded in the complex plane. In the tube with flow, the two sonic waves moving in opposite directions have different phase velocities. (According to [7] $|c_{Mi}-c|=\bar{v};\ i=1,2$, where C_{Mi} is the phase velocity with flow superimposition, c is the sonic velocity with no flow, and $\bar{v}$ is the flow velocity averaged over the cross section of the tube.) The result is a frequency-independent phase shift in the standing wave proportional to the Mach number $M = \bar{v}/c$ [3]. This fact was used for direct determination of the Mach number from the recording of the sonic pressure in the complex plane.

/ 224

3. REFLECTION FACTOR OF CROSS SECTION JUMPS AT LOW FREQUENCIES

3.1 Calculation

Powell [2] in his theory on the calculation of the reflection and transmission factors for a continuous cross section change in a tube with flow proceeds from the assumption that the flow parameters of pressure, density and velocity are

constant over the cross section, and that the flow is loss-free. The incident sonic wave allows the flow parameter behind the cross section change to fluctuate about a prescribed mean value. Let the amplitude of pressure fluctuation be $\tilde{p}_b$. Then the amplitudes of density and velocity fluctuations are $\frac{1}{c_b^2}\tilde{p}_b$ and $\frac{1}{\varrho_b c_b}\tilde{p}_b$, with ϱ_b and c_b being the density and sonic velocity behind the cross section change. If the transition length of the cross section change is small in relation to the wavelength, then one can consider the flow in the transition region as quasi-stationary. That is, the fluctuation amplitudes for the pressure, density and velocity ahead of the cross section change, $\tilde{p}_a, \tilde{\varrho}_a, \tilde{v}_a$ depend only on $\tilde{p}_b$ and the cross section ratio η ($\eta = S_a/S_b$; S_a and S_b are the cross sections before and after the cross section change). Because of the isentropy of the flow, we have automatically $\tilde{\varrho}_a = \frac{1}{c_a^2}\tilde{p}_a$. Then the reflection factor can be determined from $\tilde{p}_a/\tilde{v}_a$, the impedance of the cross section change.

With discontinuous changes in the cross section, there appear large flow losses because the flow breaks away at the edge of the cross section change, forming a jet surrounded by highly turbulent air, in the midst of stationary air. The energy in the vortices is converted into heat and removed with the flow. As the path length increases, the jet expands and finally takes up the entire cross section available. The static pressure increases along this expansion section. If one suddenly changes the flow velocity at the cross section jump, then there is a certain time until the flow has adjusted to the new equilibrium conditions and, thus, until the static pressure ahead of the expansion section has attained its new value. This response time is of the same order of magnitude as the time needed for an air particle to flow through the expansion section.

For very low frequencies, with which the period is large in relation to this response time, one can calculate the reflection factor for a discontinuous cross section change by the same method that Powell used for continuous cross section changes. As the flow is not loss-free in this case, one must also apply an entropy wave which is produced in the expansion section and flows downstream at the flow velocity. It provides that $\tilde{\varrho}_a = \frac{1}{c_a^2}\tilde{p}_a$ ahead of the cross section jump, while the corresponding quantity after the cross section jump need not be considered. Only density and temperature fluctuations appear in the entropy wave, and no pressure or velocity fluctuations. The details of this calculation are shown in the appendix.

3.2 Measurements at a perforated plate

In order to test this calculation experimentally with the available measuring system having a lower frequency limit at 0.3 kHz, it was necessary to measure an object for which the flow response time is as much smaller than 1 ms as possible. This can be done, with the given transverse dimensions for the measuring tube, only with a perforated plate. The plate used in these measurements has 54 holes of 8 mm diameter, distributed evenly across the cross section. The ratio η of hole area to the total cross sectional area is 0.48.

The course of the static pressure along the axis of the tube was measured with the microphone probe, which was connected to a U-tube manometer. The probe consisted of a tube 5 meters long (6 mm outside diameter, 1 mm wall thickness) having eight 0.8 mm holes distributed evenly around the circumference at the middle. It was placed at the axis of the 2-meter / 225 long measuring tube and held by two supports at the front and back of the measuring tube. Figure 1 shows the curve for the static pressure near the aperture plate. At the pressure minimum, A, the air jets which leave the holes and constrict

still more reach their narrowest cross section. The expansion section which follows is then clearly divided into two regions, AB and BC, with very different pressure gradients. The response time τ_B for the flow up to point B is considerably shorter than the time τ_C needed for the flow at point C to adjust to the velocity changes at the plate. Thus, the pressure

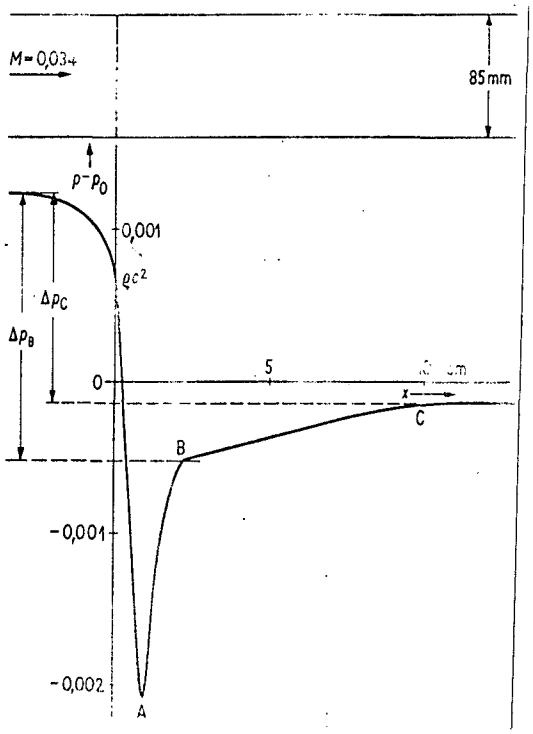

Figure 1. Example of the course of the static pressure near the perforated plate (p_0 is the external pressure).

difference Δp_C will determine the reflection factor only at very low frequencies, while at higher frequencies, where the period is comparable to τ_C but still large in comparison to τ_B, Δp_B will be decisive.

The reflection factor of the perforated plate is plotted in Figure 2 as a function of the frequency at different Mach numbers. (The Mach number always refers to the tube section ahead of the test object.) With stationary air, the reflection

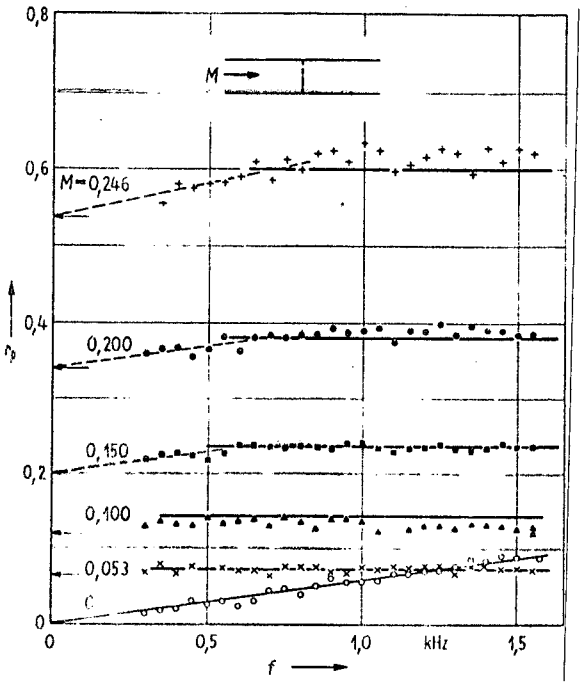

Figure 2. Reflection factor for the perforated plate as a function of the frequency, with the Mach number as parameter. The solid lines and the arrows at the flow superimposition arise from the calculation.

is due to the resonating mass of the medium, and the reflection factor increases linearly with the frequency. The plotted lines are obtained by averaging the measurements. With stationary air, the impedance is purely imaginary, within the limits of measuring accuracy. With flow superimposition, the reflection factor, in a broad frequency range, becomes independent of the frequency. Only at low frequencies does it decrease a little with decreasing frequency. The impedance is essentially real. It is determined by the differential flow resistance, while the resonating mass of the medium is to a certain extent blown away. Similar results have previously been observed by Ingard [8] for the case of large sonic amplitudes, and by Westervelt [9] as turbulence in the resonating mass of the medium. McAuliffe [10] found the same for resonators having flow through or laterally across their openings.

The solid lines at high frequencies in Figure 2 arise from the calculation described above if we use Δp_{ii} . The arrows at f = 0 arise from use of Δp_{ζ} . The dashed lines are intended to indicate the transition between the two frequency ranges. Agreement between calculation and experiment is quite good. The frequency at which the reflection factor curve bends downward should rise somewhat proportionally to the flow velocity, as the response time for the flow is inversely proportional to the flow velocity. The measuring accuracy is not great enough to confirm this, but an increase of this frequency with the Mach number can clearly be recognized.

4. REFLECTION FACTOR OF DISCONTINUOUS CROSS SECTION EXPANSIONS AT HIGH FREQUENCIES

4.1 Measurement

Now the question arises of how the reflection factor of discontinuous cross section changes is affected by the flow if the frequency of the incident sonic wave is comparable to or greater than the reciprocal response time of the flow. The pressure gradient behind the cross section jump should then no longer have any noteworthy effect on the impedance of the cross section change. For the example of cross section expansions, this would mean that the reflection factor becomes independent of the flow velocity at high frequencies, if no new mechanism comes into force to change the reflection factor at flow superimposition.

Of the discontinuous cross section changes, expansion is most simply surveyed. Up to the cross section jump, the flow parameters are independent of the path length of the flow, if we ignore the pressure gradients caused by the tube frictional resistance. Behind the expansion there forms at first a jet / 226
of constant cross section (there are no pressure gradients from constriction, as in the example with the aperture) which finally expands to the cross section of the wide tube.

Acoustically, the cross section expansion has the advantage, in respect to the aperture, that the resonating mass of the medium is of secondary importance [11], so that the reflection factor for calm air arises simply from the cross section ratio.

For this purpose, five discontinuous cross section expansions with different cross section ratios (see Table I) were measured. Figure 3, next, shows an example for the

TABLE I
THE CROSS SECTION EXPANSIONS USED

	Cross section ratio η				
	0.42	0.50	0.59	0.68	0.78
Length of expansion section / Jet diameter	4.2	3.3	2.5	1.7	1.1

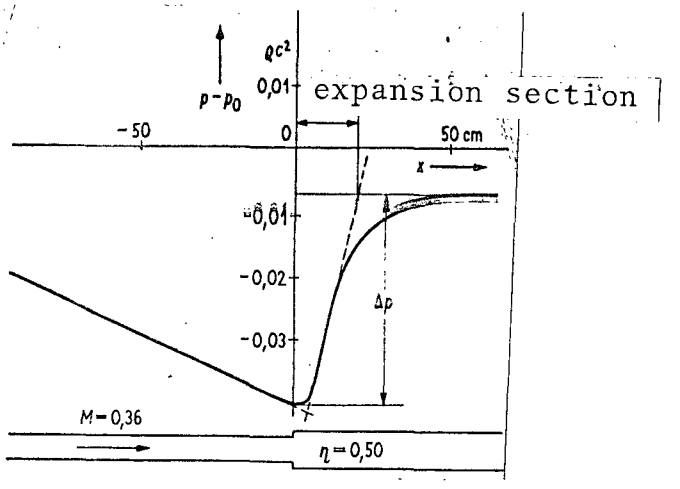

Figure 3. Course of the static pressure in a tube with flow having an expansion of the cross section.

course of the static pressure along the tube axis ($\bar{\eta}$ = 0.50). The pressure difference Δp agrees very well with the calculation (Carnot impact loss, e. g., [12]). The length of the expansion section can likewise be determined from this diagram. If one defines it in the way given there (the dashed line is the tangent through the point of inflection) it is 20 cm long in this case, and independent of the Mach number M. The corresponding lengths, in jet diameters, for the other cross section ratios are shown in Table I. (For the high Reynolds numbers of 10^5 - 10^6 which appear here, these values depend only slightly on the Reynolds number.

From the 20 cm length of the expansion section, there arises a reciprocal response time of some 170 s^{-1} at M = 0.1, and 1000 s^{-1} at M = 0.6. Accordingly, the pressure gradient should affect the acoustic reflection factor in all cases at high flow velocities and low frequencies.

Figure 4 shows the reflection factor for this discontinuous cross section expansion ($\bar{\eta}$ = 0.50) at various Mach numbers, as a function of the frequency. Each point plotted is the mean of three measurements at contiguous frequencies. For ease of viewing, the

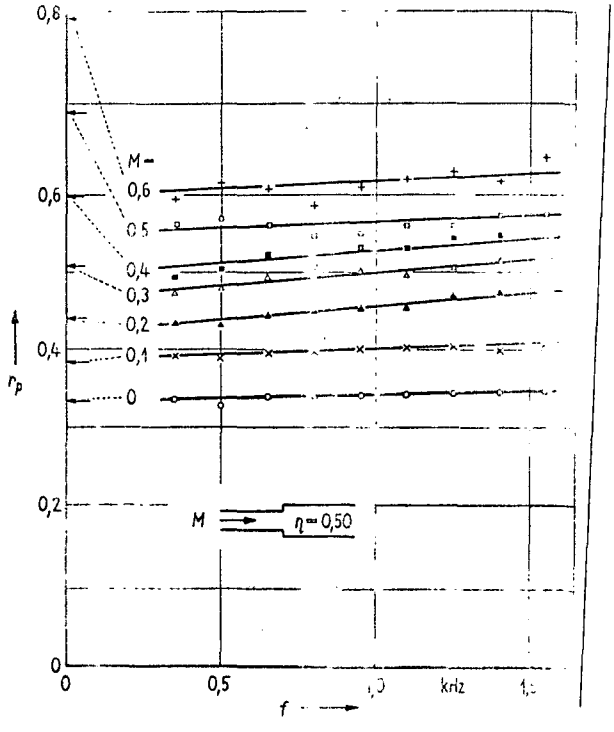

Figure 4. Reflection factor of a cross section expansion in a tube with flow as a function of the frequency, with the Mach number in the narrow tube as the parameter. The straight lines arise from averaging the measurements, and the arrows from calculations for low frequencies.

slight frequency dependence of the reflection factor is approximated here by straight lines. The measuring accuracy is not sufficient for a more exact statement. The arrows at f = 0 arise from the calculation for low frequencies (Appendix). At large Mach numbers, no transition can be detected between these calculated values and the measured ones. That means that even at low frequencies and large Mach numbers the pressure gradient behind the cross section jump has apparently no effect on the reflection factor. (This is confirmed, moreover, by another experiment described below). The agreement between calculation (for low frequencies) and measurement (at high frequencies) at low Mach numbers is obviously accidental, and does not mean that there the mechanism of the differential flow resistance / 227 is also decisive at high frequencies. This agreement is also present with all the cross section expansions measured here, as can be seen in Figure 5. There the reflection factor, because of its slight dependence on frequency, is averaged over all frequencies (0.3 kHz to 1.5 kHz) and plotted as a function of the Mach number for the various cross section ratios. The average corresponds approximately to the value measured at 0.9 kHz. For comparison, the curves calculated for low frequencies are plotted with dashed lines.

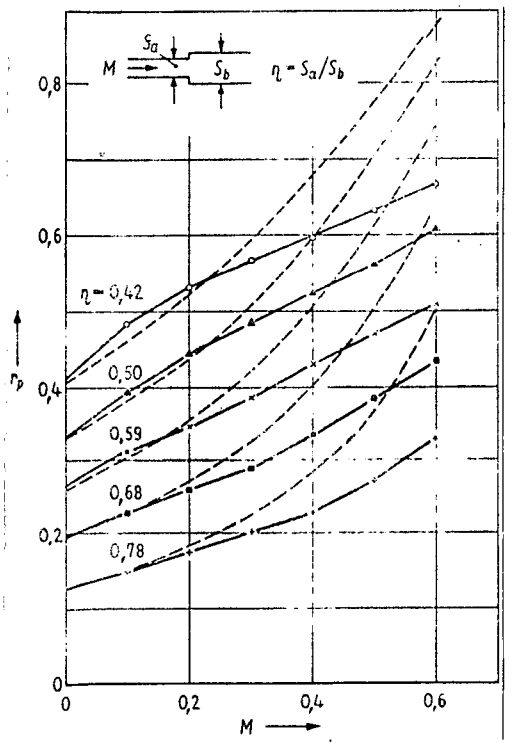

Figure 5. Reflection factor of discontinuous cross section expansions as a function of the Mach number. The cross section ratio is the parameter. (f = 0.9 kHz). The dashed curves arise from calculation for low frequencies.

The phase of the reflection factor is not measurably affected by the flow superimposition. With calm air, the resonating mass of the medium is slightly noticeable ($|\Delta\varphi_{max}| = 0.3$) but the measuring accuracy with superimposition is not high enough so that one can follow the change of the resonating mass of the medium. (In the phase measurement, the pressure gradient in the measuring section caused by the tube friction has a distinctly disturbing effect, as the density and velocity change along with the pressure, so that the internodal distance which depends on the velocity changes along the path length.) If there were an effect of the pressure gradients on the reflection factor, it should result in a strong dependence of phase on frequency, as the center of gravity of the pressure gradient section does not coincide with the cross section jump.

4.2 Directed jet

The following experiment provides a further proof that the pressure gradient behind the cross section jump does not contribute to the reflection factor of the cross sectional expansion at high frequencies. Here the narrow tube was extended into the wide tube by a 10 cm long tube of copper gauze. In this way, the air jet is directed for a distance yet, and the expansion of the jet, with the related pressure increase, first takes place after the gauze tube. Also, the flow losses become somewhat greater, so that the pressure increase is about 15% smaller than with the cross section expansion without the gauze tube.

Figure 6 shows the reflection factor for this arrangement as a function of the frequency for calm air and for flow superimposition (M = 0.3). The corresponding measurements for the same cross section expansion without the gauze tube are plotted for comparison. As expected, for calm air the gauze tube has no effect on the reflection factor, while with flow superimposition it produces a fluctuation of the reflection

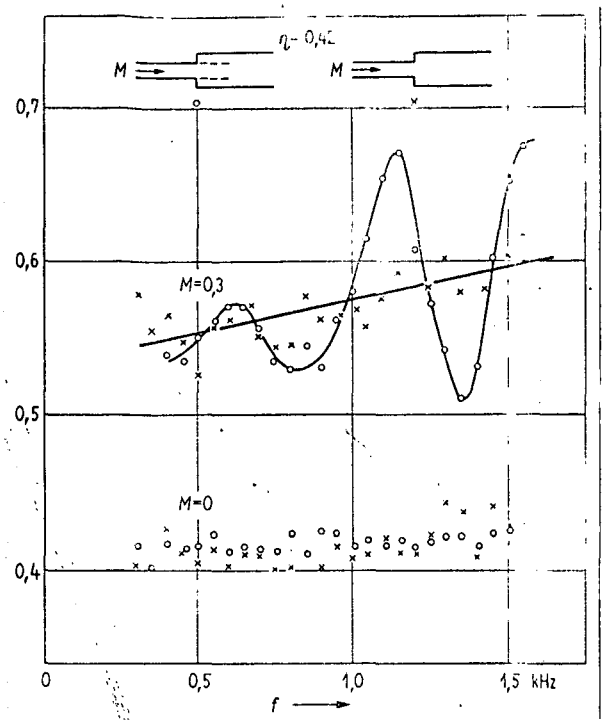

Figure 6. Reflection factor of the cross section expansion with flow, with and without the added gauze tube, as a function of the frequency. The same for calm air, for comparison.

factor which is periodic with the frequency. To be sure, the fluctuation is around the value which one obtains for the undisturbed cross sectional jump. With flow superimposition, therefore, the reflected wave is composed of two parts which interfere with each other.

From the phase of the reflection factor we can derive the fact that one – the greater – part is due to the cross section jump. This portion is equal to the wave reflected at the undisturbed cross section jump. The reflection at the cross section jump, therefore, is not changed either by the addition of the gauze tube or by the displacement and diminution of the pressure increase. Thus, it is independent of the pressure gradient. In this relation it is worth mentioning that the nature of the edge also has no noteworthy effect. Thus, rounding off of the edge (1.5 mm radius of curvature) produced only a slight increase in the reflection factor, which can be ascribed to the fact that the flow follows the curvature a little before it separates.

The second, smaller portion of the reflected wave apparently comes from the end of the gauze tube. One arrives at this result by varying the Mach number and observing the frequency separations of the reflection factor minima or maxima,

respectively. Assuming that a perturbation of the flow is produced at the cross section jump synchronously with the sonic signal, and that it moves downstream with 0.6 times the jet velocity, producing a pressure disturbance at the end of the gauze tube, which on its part moves upstream at sonic velocity and interferes with the wave reflected at the cross sectional jump, one obtains very good agreement between the measured and calculated frequency separations.

Now it will appear in the following that this flow perturbation is not only responsible for the sonic wave produced at the end of the gauze tube, but also for the change of the reflection at the cross sectional jump.

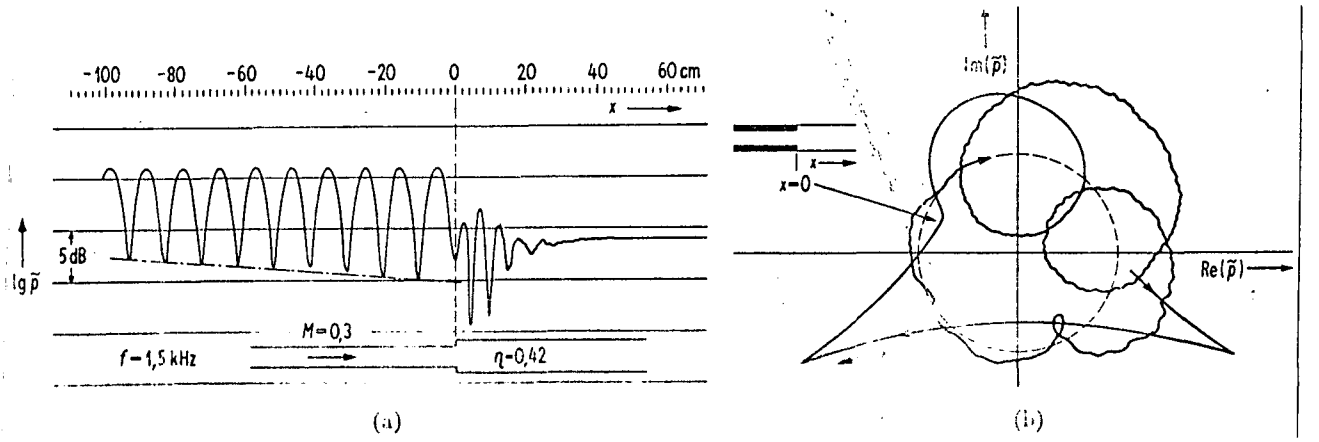

Figure 7. (a) Curve for the alternating pressure in a tube with flow, having an expansion in the cross section. (b) The same in the vicinity of the cross sectional expansion, shown in the complex plane.

4.3 Vortex wave

The flow perturbation produced at the cross sectional jump synchronously with the sound signal is already present at the cross sectional expansion without the gauze tube. Figure 7(a) shows the recording of the changing pressure amplitude along the

tube axis. The waviness behind the cross section jump is striking. Figure 7 shows how this arises. There the changing pressure curve behind the cross section jump is recorded in the complex plane, with the path length as the parameter. The dashed circle would appear if a simple sonic wave ran downstream. Obviously there is superimposed on it another wave which also runs in the positive x-direction, but which has a much higher wave number and thus a much smaller phase velocity than the sonic wave: it is equal to 0.6 times the jet velocity. Let this wave be designated as the vortex wave, because it will appear that it consists of a series of periodically detached infinitesimal ring vortices. (Blokhintsev [13] calls the phenomenon of a resting observer measuring an alternating pressure if a vortex wave passes him 'pseudosound').

The phase velocity of the vortex wave can be determined from the distances between the interference minima. Here it is assumed that the phase velocity of the sonic wave is also made up additively of the sonic velocity and of the flow velocity averaged over the cross section of the tube. It appears that the phase velocity of the vortex wave increases strongly with the path distance, and the more strongly the greater the area ratio η. The phase velocity of the vortex wave at the cross section jump is decisive for its effect on the reflection factor. This is obtained by extrapolation. It is independent of the Mach number and of the frequency. For the ratio β_0 of this extrapolated phase velocity to the jet velocity we obtain / 229

$$\beta_0 \approx 1 - \eta.$$

In Figure 8, the varying pressure behind the cross section jump is plotted at the tube axis, within the jet region (solid curve) and also at the tube wall outside the jet (dashed line) as a function of the path distance (linear scale). The alternating pressure of the vortex wave has almost identical phase across the tube cross section.

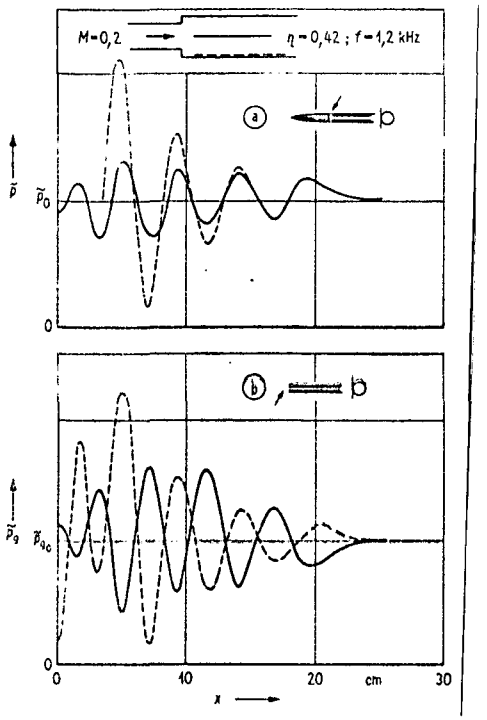

Figure 8. Course of the varying pressure (a) and the varying total pressure (b) in the jet axis (——) and at the edge of the tube (- - -). $\tilde{p}_0'$ and $\tilde{p}_{g_0}$ are the corresponding quantities for the sound wave.

From the momentum equation for the flow, assumed to be frictionless,

$$\varrho \frac{Dv}{Dt} + \operatorname{grad} p = 0 \qquad (1)$$

(ρ = medium density; Dv/Dt = hydrodynamic derivative with respect to time; p = pressure) the speed distribution in the vortex wave can be derived. For this we make in addition the simplified assumption that the profile of the velocity is rectangular. That is, that the velocity is $\bar{v}$ = Mc across the entire cross section of the jet, and zero outside it. Then for the velocity component in the axial direction, v_x, in the jet region after linearization, we have

$$\varrho\left(\dot{v}_x + \bar{v}\frac{\partial v_x}{\partial x}\right) + \frac{\partial p}{\partial x} = 0 \qquad (2a)$$

and outside this region

$$\varrho \dot{v}_x + \frac{\partial p}{\partial x} = 0. \qquad (2b)$$

Here the varying component of p is still a function of the radius, but that is of no importance for this consideration. Now if we introduce the fact that the varying quantities depend on time and place according to the wave factor $\mathrm{j}(\omega t - k_W x)$ (ω = rotational frequency, k_W = wave number of the vortex waves), we obtain

$$\tilde{v}_{Wx} = \tilde{p}_W \frac{k_W}{\varrho\omega - \varrho k_W \bar{v}} = -\frac{\tilde{p}_W}{\varrho c} \frac{1}{M(1-\beta)} \qquad (3a)$$

in the jet region and

$$\tilde{v}_{Wx} = \tilde{p}_W \frac{k_W}{\varrho\omega} = \frac{\tilde{p}_W}{\varrho c} \frac{1}{M\beta}, \qquad (3b)$$

outside. Here $\tilde{p}_W$ and $\tilde{v}_{Wx}$ are the varying amplitudes of pressure and axial velocity in the vortex wave, and β is the ratio of the phase velocity to the jet velocity.

Because β is always less than 1, the pressure and velocity are of opposite phase in the jet region and of the same phase outside. The phase opposition in the jet region can be confirmed by measuring the alternating component of the total pressure p_g there with a microphone having its sound pickup opening at the stagnation point. (Probe microphone with a probe open at the front. As the probe diameter is small in comparison to the vortex wavelength, we can neglect the non-steady term in the Bernoulli equation which corresponds to the oscillating mass of the medium ahead of the probe opening.) For the case of small Mach numbers, and using Equation (3a), we obtain for the varying total pressure of the vortex wave in the jet region

$$\tilde{p}_{gW} = \tilde{p}_W + \left(\frac{\varrho}{2} \tilde{v}^2_{Wx}\right) = \tilde{p}_W \left(1 + \frac{M^2}{2}\right) + M\varrho c \tilde{v}_{Wx} \approx \tilde{p}_W \frac{\beta}{1-\beta}. \qquad (4)$$

Thus, the varying components of the static and total pressure there are in phase opposition, while of course $\tilde{p}_{gW} = \tilde{p}_W$ outside the jet. Figure 8b shows this, where the curves for the varying total pressure inside (solid line) and outside (dashed line) the jet are plotted, in comparison with Figure 8a.

/ 230

According to these deliberations, one can conceive of the vortex wave rather as a periodic sequence of infinitesimal ring vortices with alternating directions of rotation, which are superimposed upon the steady flow and which are detached at the cross section jump synchronously with the sound signal.

The vortex wave is next strengthened along its path until it comes to the region where the jet begins to expand, so that it no longer encounters suitable expansion conditions. The vortex wave can be observed even far behind the cross sectional jump, especially with large cross sectional ratios, n, with which the expansion section is rather short. Apparently the velocity profile of turbulent tube flow is a sufficient expansion condition for a vortex wave excited at a relatively small step in the cross section.

4.4 Effect of the vortex wave on the reflection factor

Now the following hypothesis for the mechanism of the reflection change at a discontinuous cross section expansion by superimposition of a flow at high frequencies arises:

The air jet at the cross section mump is modulated by the speed of sound; thus, a vortex wave is produced, having a speed in the jet region which is of the same phase as the sonic wave. The oppositely phased varying pressure of the vortex wave is subtracted from the sonic pressure (in Figure 8a there is a minimum in the total varying pressure at $x = 0$). In this way the impedance of the cross section expansion is also diminished. As this impedance is already smaller than the wave resistance without the presence of a vortex wave, the contribution to the reflection factor increases with further diminution. The amount by which the impedance of the cross section jump decreases depends on how strongly the vortex wave is excited. The excitation factor arises from the boundary conditions. In this respect, it is worth mentioning that to the boundary condition which applies in calm air, i. e., the disappearance of the axial component of speed for $x = 0$, $a < r \leq b$ (Figure 9) [14, 11] there is added another one. This is the disappearance of the radial component of the speed for $x = 0$, $r = a$ in a wider tube. In calm air, the speed-flow lines near the walls follow the contours of the cross sectional jump. (In the upper

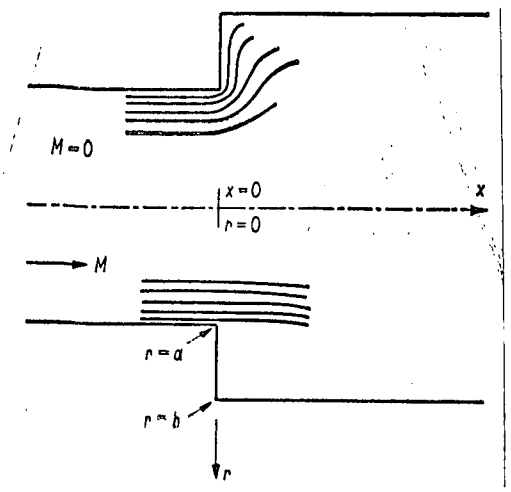

Figure 9. On the boundary conditions for the acoustic flow variation in the vicinity of a cross section expansion.

part of Figure 9 this curve of flow lines is drawn qualitatively.) If the viscosity is neglected, the speed at the edge even becomes infinitely large. With flow superimposition, however, it must follow the contours of the air jet (Figure 9, lower part). In order to meet the boundary conditions exactly, one naturally requires the higher modes of sonic expansion and probably also higher modes of the vortex wave.

It still remains to be investigated whether this hypothesis on the mechanism of the reflection change at high frequencies agrees with the measurements: As the radial speed must vanish at $x = 0$ and $r = a$ (Figure 9), the flow field near the cross section jump is not changed by addition of the gauze tube. The gauze tube should also not notably disturb the excitation of the vortex wave. The wave number of the vortex wave also does not change, because the value $\beta_0 = 0.6$ had appeared for the cross section change without the added gauze tube, and for the cross section expansion with the gauze tube we likewise obtained the value of 0.6 for β from the frequency separations of the reflection factor maxima. So it is no wonder that the gauze tube does not affect the reflection factor at the cross section jump.

If we assume that the structure of the vortex wave, i. e., its speed and pressure distribution across the tube cross section, does not depend strongly upon the Mach number, as is suggested by the fact that β is independent of the Mach number within the

limits of measuring accuracy, then its excitation strength, referred to the speed, should also not depend strongly on the Mach number (the speed at the cross section jump is the decisive quantity in the excitation of the vortex wave). Then, according to Equation (3), the varying pressure of the vortex wave is proportional to the Mach number and the impedance of the cross section jump is a linear function of the Mach number. As a first approximation, then, the reflection factor is also linearly dependent on the Mach number. This agrees with the measurement (Figure 5).

The phase of the reflection factor does not significantly / 231
deviate from 180°. If we ignore the higher modes which are excited at the cross section jump but which are not capable of propagation, therefore, the varying pressure at the cross section jump should be about equal to the sonic pressure in the minima of the standing wave in the narrow tube. But at high frequencies in particular, it is considerably greater than the sonic pressure at the minima. The deviation, referred to the varying pressure of the vortex wave at the cross section jump, decreases with increasing vortex wavelength. This deviation results from the fact that the varying pressure of the vortex wave increases strongly in the radial direction, especially at the cross section jump (Figure 8a) and that the sonic wave reflected there to a certain extent averages the varying pressure over the entire cross section of the narrow tube. Thus, it has a higher amplitude than would correspond to the varying pressure in the tube axis at the cross section jump. The varying pressure changes especially strongly in the radial direction, of course, if the vortex wave length is small in comparison to the tube radius.

To confirm that, the varying pressure at the edge of the jet was recorded as a function of the axial coordinate x at various frequencies and Mach numbers. The result is summarized in Figure 10. The Mach number increases to the right, and the frequency increases upward. In the individual parts of the

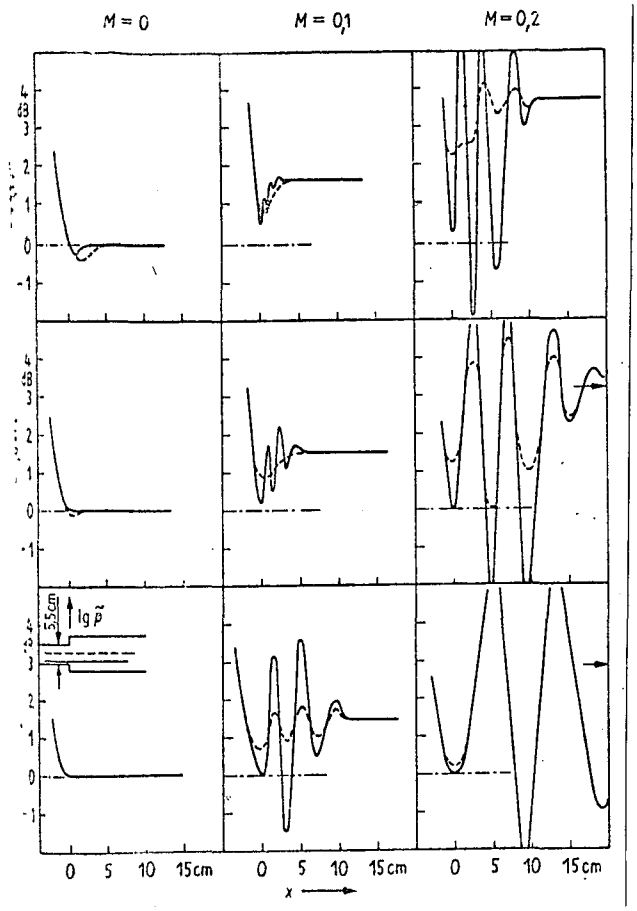

Figure 10. Curve of the alternating pressure in the vicinity of the cross section expansion with flow at the edge of the jet (——) and in the jet axis (---) for various frequencies and Mach numbers.

figure, the alternating pressure at the edge of the jet is represented by the solid lines and that in the axis of the jet by the dashed lines. The dot-dash line always shows the sonic pressure of the minima in the narrow tube. From this figure we can estimate that the average alternating pressure at $x = 0$ is approximately equal to the sonic pressure at the standing wave minima only for large vortex wavelengths. With decreasing vortex wave length, however, it becomes steadily more clearly recognizable that still another mechanism participates in the reflection change due to flow superimposition. If its wavelength is small in comparison to the diameter of the narrow tube, the vortex wave makes no contribution to the reflected sound wave. Its range of action, then, is limited essentially to the edge of the jet. The boundary conditions are fulfilled only by the sonic modes.

The frequency range within which the vortex wave produces the essential part of the flow-conditioned reflection factor change of the discontinuous cross section expansion is given by the conditions that the vortex wavelength must be

smaller than or comparable to the length of the expansion section behind the cross section jump and larger than or comparable with the diameter of the narrow tube.

4.5 Opening, with flow, in an infinitely large wall

If we allow the cross section ratio $\bar{n}$ at the discontinuous cross section expansion to approach zero, then in the limiting case the narrow tube discharges into half-space, and one obtains the opening with flow in an infinitely large wall. (With this boundary transition, to be sure, the requirement that only the ground mode be capable of propagation even in the "wide tube" is omitted.) This case has already been studied in [7]. Here we wish to make a contribution to explaining the measurements obtained there. Figure 11 shows once more the reflection factor of an opening, with flow, in a wall as a function of the frequency parameters ka ($k = \omega/c$ = wavenumber, 2a = diameter of the opening) for various Mach numbers. At the frequency of zero it has the value of 1, independent of the Mach number. It becomes larger with increasing frequency, reaching a maximum at a frequency which is about proportional to the Mach number. At higher frequencies, then, we have $r_p(ka, M) \approx r_p(ka, 0)m(M)$, where r_p is the reflection factor and m(M) is a function depending only on M. At low Mach numbers, we have $m(M) \approx 1 + 2M$. / 232

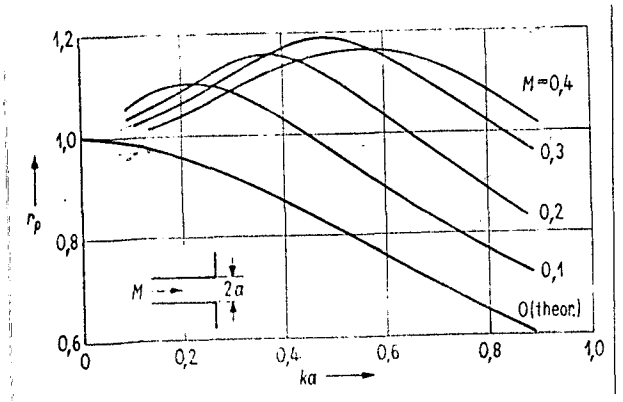

Figure 11. Reflection factor of the opening, with flow, in an infinite wall as a function of ka, with the Mach number as parameter.

Here, too, the increase in the reflection factor can be traced back to the excitation of a vortex wave. Figure 12 shows an example for the course of the alternating pressure in the axial direction of the tube, measured at the edge of the tube or jet, respectively, and shown in the complex plane. The vortex wave is very strongly

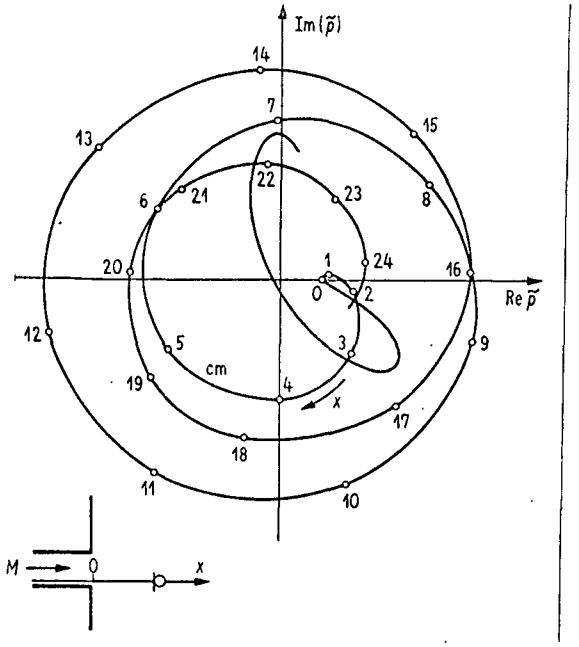

Figure 12. Curve of the alternating pressure at the edge of a free jet, shown in the complex plane. M = 0.3, f = 0.75 kHz.

developed in this case, so that the sonic wave can be neglected in comparison with it, except in the vicinity of the opening. The vortex wave in the free jet agrees in its essential properties with the vortex wave in the tube. In the jet region the alternating pressure and the alternating total pressure are of opposite phase. The amplitude of the alternating pressure is greater at the edge of the jet than in its axis.

For the frequency-Mach number combination shown in Figure 12, the reflection factor of the opening has just one maximum as a function of the frequency. It appears that at this frequency - Mach number combination the vortex wave is particularly strongly developed. The vortex wave length is about equal to the diameter. With constant Mach number and decreasing frequency, the amplitude of the vortex wave decreases in about the same amount as the reflection factor approaches the value of 1, while the amplitude curve along the flow path remains similar. Also with increasing frequency, one finds a decrease of the vortex wave amplitude, while the sonic wave behind the opening becomes steadily stronger, and is finally dominant. Like the amplitude of the vortex wave, β also depends on the frequency. At the frequency at which the reflection factor has its maximum, β takes on its smallest value of 0.5 . . . 0.6 (the value decreases somewhat with increasing Mach number). At high and low frequencies β increases to about 0.8. These values apply directly behind

the opening. With increasing flow path, β likewise increases.

The fact that the reflection factor has the value of 1 at zero frequency, independent of the Mach number, can be explained as follows. Here the impedance change due to the flow is given by the differential flow resistance which vanishes at $\eta = 0$. With increasing frequency, a vortex wave forms, with simultaneous increase in the reflection factor. Here there is a noticeable difference from the cross section expansion in a tube, where this increase of the reflection factor with frequency does not appear at low frequencies. One possible explanation for it is the fact that when η is not too small, the vortex wave fills the entire cross section of the wide tube, so that the alternating pressure cannot expand transverse to the jet, as with very small η (especially with $\eta = 0$). If the maximum of the vortex wave excitation and so of the reflection factor is exceeded and the vortex wavelength becomes small in relation to the opening diameter, the effect of the vortex wave on the reflection factor moves into the background as with the cross section expansions.

Vortex detachment synchronized by sonic irradiation has previously been studied by Wehrmann [15] on a laminar round free jet. He measured the vortex wave with a hot wire anemometer. The vortex wave also plays a decisive role in relation to whistle tones in systems in which a laminar free jet strikes an appropriate barrier [16, 17]. Among other things, von Gierke [16] measured the wave length of the vortex wave by means of two alternating pressure probes. He also found / 233
the vortex to be most distinct if the wave length was about equal to the jet diameter. Chanaud and Powell [17] obtained for the vortex wave in a laminar free jet (maximum Reynolds number = 4,000) a decrease in the phase velocity with the flow distance, in opposition to the observations made here on turbulent jets.

Some concluding comments on the acoustic energy which is stored in the vortex wave at the cross section jump: this energy is converted to heat on the collapse of the vortex; that is, in general, the excitation of the vortex wave represents an acoustic loss mechanism if no more acoustic energy can be regained from the amplified vortex wave after a certain path distance than was needed for its excitation. Examples for the recovery of acoustic energy are the experiment with the gauze tube (Section 4.2), sound amplification in channels which are covered with Helmholtz resonators at periodic separations [18] and especially the self-excited whistling of jet-barrier systems [16, 17].

5. CONCLUDING REMARKS

For discontinuous cross section changes and for apertures in a tube with flow, a formula has been derived with which one can use the velocity-dependent drop of the static pressure at these flow barriers to calculate the acoustic reflection factor at low frequencies. This calculation is an extension of Powell's theory [2] for calculation of the reflection factors of continuous cross section changes. The formula reproduces the measurements correctly as long as the flow behaves as quasi-stationary in the vicinity of the cross section jump, while at higher frequencies a new mechanism determines the acoustic properties of the discontinuous cross section change.

With the example of discontinuous cross section expansions it is shown that we are dealing with excitation of a vortex wave which consists of a periodic sequence of infinitesimal ring vortices. These are detached from the edge of the cross section jump synchronously with the sonic signal. The vortex wave is detectable through its alternating pressure, and can be differentiated well from the sonic wave because of its quite different phase velocity. The alternating pressure and speed of the vortex wave have the same phase in the region of the air jet which forms behind the cross section expansion. The vortex

speed in the jet region and the sound speed are of the same phase at the cross section jump, so that the alternating pressure of the vortex wave is subtracted from the sonic pressure. In this way the impedance of the cross section expansion is decreased. This leads to increase of the reflection factor. For the case of low Mach numbers (up to M = 0.2) the change in the reflection factor is equally large at low and high frequencies. It also appears that the vortex wave is no longer responsible for the flow-produced reflection change at frequencies for which its wave length is small in comparison to the diameter of the narrow tube.

The results found for cross section expansions can be applied to the case in which a tube discharges in an infinitely large wall. Application to apertures and discontinuous constrictions in a tube, however, is not immediately possible, as here there appears a strong pressure gradient directly at the cross section jump, because of the jet contraction. In addition, no vortex wave is capable of propagation at the cross section jump with a constriction. Correspondingly, it is only weakly developed behind it. For the case of an aperture, Figure 13 shows that the reflection factor behaves qualitatively differently than for the cross section expansion. For this, according to Powell [2], that portion of the reflection factor which results from the tube cross section narrowing to the aperture cross section was calculated. Then, from the measured reflection factor, one can determine the reflection

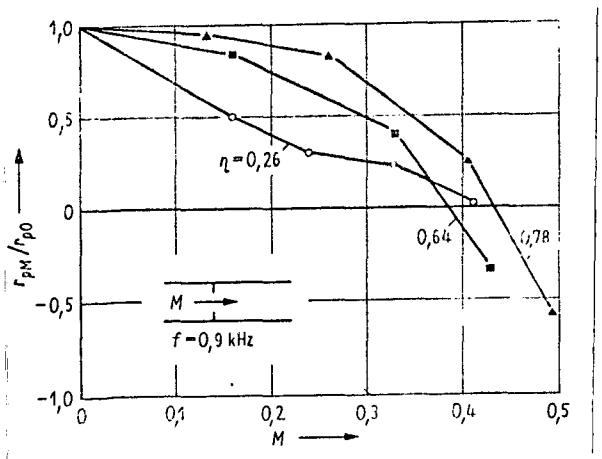

Figure 13. Reflection factor, normalized to M = 0 for the discontinuous cross section expansion behind an aperture as a function of the Mach number for various cross section ratios.

factor of the following cross sectional expansion. It is plotted in Figure 13 for three different apertures, as a function of the Mach number in the aperture cross section, and normalized to the corresponding value for calm air. It appears that it drops sharply with increasing Mach number, in contrast to the reflection factor of the normal discontinuous cross section expansion. /234

I thank Prof. Dr. phil. Dr. Ing. E. h. E. Meyer for suggesting this work and for participating in its performance. Dr. E. A. Müller and his colleagues also deserve my thanks for discussion of the theoretical aspects of the theme.

APPENDIX

Calculation of the reflection factor of discontinuous cross section changes and apertures in a tube with flow at low frequencies for the case in which the incident wave moves in the direction of flow:

It is assumed that the flow parameters are constant across the tube cross section. Also, the pressure drop at the cross section change or aperture is considered to be only a function of the Mach number ahead of the cross section change or aperture, respectively. Therefore, we neglect the effect of the Reynolds number on the pressure drop, as we are dealing here with very large Reynolds numbers. The medium is considered an ideal gas. The symbols for the parameters ahead of or behind the cross section jump are indexed with a or b, respectively.

The applicable equations are the continuity equation

$$\eta v_a \varrho_a = v_b \varrho_b , \tag{A1}$$

the energy equation

$$\frac{v_a}{2} + \frac{\gamma}{\gamma-1}\frac{p_a}{\varrho_a} = \frac{v_b}{2} + \frac{\gamma}{\gamma-1}\frac{p_b}{\varrho_b} \tag{A2}$$

and the momentum equation in the form

$$p_a P(M_a^2) = p_b, \tag{A3}$$

in which $P(M_a^2)$ must be measured. (p is the pressure, ρ the density, v the velocity, $M^2 = (v^2\varrho)/(\gamma p)$, the square of the Mach number, γ the ratio of the specific heats, and η the ratio of the cross sections ahead of and behind the cross section jump.) p, ρ, and v are varied by the sound wave. With the sound quantities designated by ~, and with the quantities for the incident and reflected waves indexed with 1 or 2, respectively, we obtain for superimposition of a sound wave in the direction of flow

$$\begin{aligned} p_a &\to p_a + \tilde{p}_1 + \tilde{p}_2 & p_b &\to p_b + \tilde{p}_b \\ \varrho_a &\to \varrho_a + (1/c_a^2)(\tilde{p}_1 + \tilde{p}_2) & \varrho_b &\to \varrho_b + (1/c_b^2)(\tilde{p}_b + \tilde{\sigma}) \\ v_a &\to v_a + (1/\varrho_a c_a)(\tilde{p}_1 - \tilde{p}_2) & v_b &\to v_b + (1/\varrho_b c_b)\tilde{p}_b \end{aligned} \tag{A4}$$

Here $(1/c_b^2)\tilde{\sigma}$ is the density amplitude of the entropy wave (see Section 3.1) and c is the speed of sound. If we insert Equation (A4) into Equations (A1), (A2), and (A3), eliminating the constant quantities, then after linearization we obtain

$$\eta[\tilde{p}_1(1+M_a) - \tilde{p}_2(1-M_a)](c_b/c_a) = \tilde{p}_b(1+M_b) + \tilde{\sigma}\,M_b \tag{A5}$$

$$[\tilde{p}_1(1+M_a) + \tilde{p}_2(1-M_a)](c_b/\varrho_a) = \tilde{p}_b(1+M_b) - \frac{1}{\gamma-1}\tilde{\sigma} \tag{A6}$$

$$(M_a/\gamma)P'[\tilde{p}_1(2-(\gamma-1)M_a)- -\tilde{p}_2(2+(\gamma-1)M_a)]+P(\tilde{p}_1+\tilde{p}_2)=\tilde{p}_b \tag{A7}$$

Here $P'=\dfrac{dP(M_a^2)}{d(M_a^2)}$ and $dM_a^2=M_a^2\left(\dfrac{2\,dv_a}{v_a}+\dfrac{d\varrho_a}{\varrho_a}-\dfrac{dp_a}{p_a}\right)$.

The reflection factor is given by $r_p=\tilde{p}_2/\tilde{p}_1$, and if we set $M_b(\varrho_b/\varrho_a)=\eta M_a(c_a/c_b)$, we obtain

$$r_p=\frac{\eta\left(\dfrac{1}{\gamma-1}\dfrac{c_b}{c_a}+M_a\dfrac{c_a}{c_b}\right)(1+M_a)-\left[\dfrac{M_a}{\gamma}P'(2-(\gamma-1)M_a)+P\right]\left(\dfrac{1}{\gamma-1}+M_b\right)(1+M_b)}{\eta\left(\dfrac{1}{\gamma-1}\dfrac{c_b}{c_a}-M_a\dfrac{c_a}{c_b}\right)(1-M_a)-\left[\dfrac{M_a}{\gamma}P'(2+(\gamma-1)M_a)-P\right]\left(\dfrac{1}{\gamma-1}+M_b\right)(1+M_b)} \tag{A8}$$

From Equations (A1), (A2) and (A3) we obtain

$$M_b^2=\frac{1}{2\vartheta}\left(\sqrt{1+4\vartheta\eta^2M_a^2\frac{1+M_a^2}{P^2}}-1\right), \tag{A9}$$

in which $\vartheta=(\gamma-1)/2$. For air, $\vartheta=0.2$. For the case in which $4\eta^2M_a^2\,\dfrac{1+M_a^2}{P^2}\ll 1$, then

$$M_b\approx\frac{\eta M_a}{P}\left[1+(\vartheta/2)M_a^2\left(1-\frac{\eta^2}{P^2}\right)\right]$$
$$\frac{c_b}{c_a}\approx\frac{M_b}{M_a}P\approx 1+(\vartheta/2)M_a^2\left(1-\frac{\eta^2}{P^2}\right). \tag{A10}$$

For an aperture, η is to be set equal to 1. For the case of incompressible flow, in which $P\approx 1$, $M_b=\eta M_a\ll 1$, Equation (A8) simplifies to

$$r_p\approx\frac{[\eta-(2M_a/\gamma)P']-1}{[\eta-(2M_a/\gamma)P']+1}. \tag{A11}$$

If we also consider that in this case $-(2M_a/\gamma)P'\varrho c$ is exactly the differential flow resistance $d(\Delta p)/dv_a$ (Δp is the pressure drop at the cross section jump), then we see from Equation (A11) that the impedance of the cross section jump with flow arises as the sum of the impedance of the cross section jump with calm air, $\eta\varrho c$ and the differential flow resistance [1].

If we deal with a cross section expansion ($\eta < 1$), then P can be calculated from the momentum equation (e. g., [12]). Then Equation (A3) becomes

$$\varrho_a v_a^2 \eta + p_a = \varrho_b v_b^2 + p_b . \qquad \text{(A3a)}$$

Then, along with Equations (A1), (A2) and (A4), we obtain

$$r_p = \frac{(1+M_a)\frac{c_b}{c_a}\left[\frac{1}{\gamma-1}(1+M_b)+M_b^2+\left(\frac{c_a}{c_b}\right)^2 M_a\right]-\left(\frac{1}{\gamma-1}+M_b\right)\left(\frac{1}{\eta}+2M_a+M_a^2\right)}{(1-M_a)\frac{c_b}{c_a}\left[\frac{1}{\gamma-1}(1+M_b)+M_b^2-\left(\frac{c_a}{c_b}\right)^2 M_a\right]+\left(\frac{1}{\gamma-1}+M_b\right)\left(\frac{1}{\eta}-2M_a+M_a^2\right)} . \qquad \text{(A8a)}$$

Here the relation $(c_b/c_a)^2 = 1+\vartheta M_a^2\left[1-\left(\frac{v_b}{v_a}\right)^2\right]$ applies; therefore,

$$\begin{aligned} \frac{c_b}{c_a} &\approx 1+\frac{\vartheta}{2}M_a^2\left[1-\left(\frac{v_b}{v_a}\right)^2\right] \\ M_b &\approx M_a\frac{v_b}{v_a}\left[1-\frac{\vartheta}{2}M_a^2\left(1-\left(\frac{v_b}{v_a}\right)^2\right)\right], \end{aligned} \qquad \text{(A10a)}$$

in which we obtain the value for v_b/v_a from the expression given in [12]

$$v_b/v_a = \eta[1+(1/2)(1-\eta)\ (\gamma-1-\eta(\gamma+1))M_a^2 \\ (1-\eta(\gamma-\eta(\gamma+1))\ M_a^2)]$$

if we expand the root according to M_a^2 and terminate after the third term.

For incompressible flow, we obtain

$$r_p = \frac{[\eta + M_a(\eta - 1)2\eta] - 1}{[\eta + M_a(\eta - 1)2\eta] + 1} \cdot \Big| \qquad \text{(A11a)}$$

REFERENCES

1. Lutz, O. Berichte aus dem Laboratorium für Verbrennungskraftmaschinen der TII Stuttgart (Report from the Combustion Engine Laboratory of the Stuttgart Technical University), Vol. 3, 1934, p. 17.

2. Powell, A. J. Acoust. Soc. Amer., Vol. 31, 1959, p. 1527; Vol. 32, 1960, pp. 1116 and 1640.

3. Ronneberger, D. and W. Schilz. Acustica, Vol. 17, 1966, p. 168.

4. Sivian, L. J. J. Acoust. Soc. Amer., Vol. 7, 1935, p. 94.

5. Westervelt, P. J. and P. W. Sieck. J. Acoust. Soc. Amer., Vol. 22, 1950, p. 680.

6. Barthel, F. Frequenz, Vol. 12, 1958, p. 72.

7. Mechel, F., W. Schilz and J. Dietz. Acustica, Vol. 15, 1965, p. 199.

8. Ingard, U. and S. Labate. J. Acoust. Soc. Amer., Vol. 22, 1950, p. 211; Ingard, U. J. Acoust. Soc. Amer., Vol. 25, 1953, p. 1037.

9. Westervelt, P. J. J. Acoust. Soc. Amer., Vol. 23, 1951, p. 347.

10. McAuliffe, C. E. M.I.T., M. S. Thesis, Massachusetts, 1950.

11. Karal, F. C. J. Acoust. Soc. Amer., Vol. 25, 1953, p. 327.

12. Oswaltitsch, K. Gasdynamik (Gas Dynamics), Springer Verlag, Wien, 1952.

13. Blokhintsev, D. I. NACA TM 1399 , Übersetzung.

14. Miles, J. W. J. Acoust. Soc. Amer., Vol. 16, 1946, p. 14.

15. Wehrmann, O. DVL-Bericht 131; Jahrbuch 1957 der WGL (DVL Report 131; 1957 Yearbook of the WGL , p. 102.

16. v. Gierke, H. Z. angew. Phys., Vol. 2, 1950, p. 97.

17. Chanaud, R. C. and A. J. Powell. J. Acoust. Soc. Amer., Vol. 37, 1965, p. 902.

18. Meyer, E., F. Mechel and G. Kurtze. J. Acoust. Soc. Amer., Vol. 30, 1958, p. 165. Mechel, F. Acustica, Vol. 10, 1960, p. 133.

Translated for National Aeronautics and Space Administration under contract No. NASw 2035, by SCITRAN, P.O. Box 5456, Santa Barbara, California, 93108